Generalized Measurable Ignition Criterion for Inertial Confinement Fusion

PY. Chang,[1,2] R. Betti,[1,2] B. K. Spears,[3] K. S. Anderson,[1,2] J. Edwards,[3] M. Fatenejad,[4] J. D. Lindl,[3] R. L. McCrory,[1] R. Nora,[1,2] and D. Shvarts[5]

[1]*Laboratory for Laser Energetics, University of Rochester, Rochester, New York 14623, USA*
[2]*Fusion Science Center for Extreme States of Matter, University of Rochester, Rochester, New York 14623, USA*
[3]*Lawrence Livermore National Laboratory, Livermore, California 94550, USA*
[4]*Department of Engineering Physics, University of Wisconsin, Madison, Wisconsin 53706, USA*
[5]*NRCN, Negev and Ben Gurion University of the Negev, Beer-Sheva, 84015, Israel*
(Received 5 January 2010; published 1 April 2010)

A multidimensional measurable criterion for central ignition of inertial-confinement-fusion capsules is derived. The criterion accounts for the effects of implosion nonuniformities and depends on three measurable parameters: the neutron-averaged total areal density ($\rho R_n^{\rm tot}$), the ion temperature (T_n), and the yield over clean (YOC = ratio of the measured neutron yield to the predicted one-dimensional yield). The YOC measures the implosion uniformity. The criterion can be approximated by $\chi = (\rho R_n^{\rm tot})^{0.8} \times (T_n/4.7)^{1.7}{\rm YOC}^{\mu} > 1$ (where ρR is in g cm^{-2}, T in keV, and $\mu \approx 0.4$–0.5) and can be used to assess the performance of cryogenic implosions on the NIF and OMEGA. Cryogenic implosions on OMEGA have achieved $\chi \sim 0.02$–0.03.

DOI: 10.1103/PhysRevLett.104.135002 PACS numbers: 52.57.Bc, 52.57.Fg

In inertial-confinement fusion (ICF) [1], a shell of cryogenic deuterium and tritium (DT) thermonuclear fuel is accelerated inward by direct laser irradiation or by the x rays produced by heating a high-Z enclosure (hohlraum). At stagnation, the compressed fuel is ignited by a central hot spot surrounded by a cold, dense shell. Central ignition occurs when the alpha-particle heating of the hot spot exceeds all the energy losses. To measure progress toward ignition, a metric is needed to assess how an implosion experiment performs with respect to the ignition condition. In a stationary plasma, the ignition condition is given by the Lawson criterion [2]. In ICF, the same ignition condition must be derived in terms of measurable parameters. Different forms of the 1-D ignition condition have been derived [1,3,4] but none of them can be accurately measured. Measurable parameters of the ICF fuel assembly are the total areal density, the ion temperature, and the neutron yield. In this Letter, we show that the ignition condition can be written in terms of these measurable parameters. We start from the 1-D ignition model of Ref. [5] and generalize it to multidimensions through a single parameter: the yield over clean or YOC. The YOC is the ratio of the measured neutron yield to the predicted 1-D yield. The latter must be calculated consistently with the measured ρR and T_i. The generalized ignition criterion depends on the total areal density, the ion temperature, and the YOC.

This Letter has two parts. The first deals with the 3-D extension of the dynamic ignition model [5,6] and an analytic ignition criterion. The second shows the results of hydrodynamic simulations of imploding capsules forming the database used to generate a more accurate ignition condition. A measurable criterion requires the solution of a dynamic ignition model. The analysis starts by modifying the 1-D ignition model {Eqs. (15) of Ref. [5]} and the following considerations about multidimensional effects. The hot spot is enclosed by the surrounding shell that can be highly distorted by hydrodynamic instabilities. The hot-spot volume is bounded by the Rayleigh-Taylor (RT) bubbles and spikes from the shell. The plasma in the bubbles is cold and does not contribute to the fusion yield. Following the analysis of Ref. [7], we assume that only the "clean" hot-spot volume $V_{\rm clean}$ within the RT spikes [Fig. 1] is hot enough to induce fusion reactions, and the central temperature is unchanged by the RT evolution as long as the RT spikes do not reach the hot-spot center. The 1-D ignition model can be extended to 3-D by integrating the alpha-particle energy deposition over the clean hot-spot volume leading to

$$\frac{d}{d\tau}(\hat{P}\hat{R}^3) = -2\hat{P}\hat{R}^2\frac{d\hat{R}}{d\tau} + \gamma_\alpha \hat{P}^2\hat{T}\hat{R}^3_{\rm clean}, \tag{1}$$

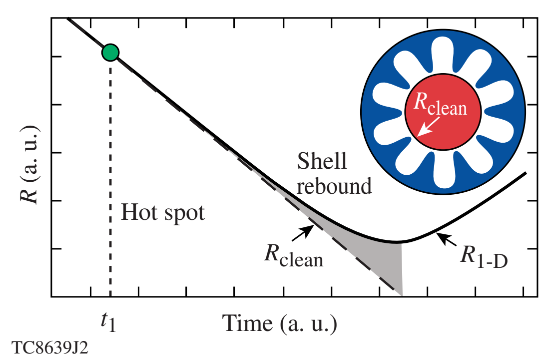

FIG. 1 (color online). Schematic of the free-fall model. Fusion reactions occur only in the clean volume within the Rayleigh-Taylor spikes. The spikes "free fall" after saturation of the linear growth.

$$\frac{d}{d\tau}\left(\frac{\hat{P}\hat{R}^3}{\hat{T}}\right) = \hat{R}\hat{T}^{5/2}, \qquad (2)$$

$$\frac{d^2\hat{R}}{d\tau^2} = \hat{P}\hat{R}^2. \qquad (3)$$

With respect to the 1-D case, the alpha heating is reduced by the clean-volume fraction $R_{\rm clean}^3/R^3$, where $R_{\rm clean}$ and R are the clean and 1-D radii, respectively. We assume this to be the main effect of the implosion nonuniformities. In Eqs. (1)–(3), the hot-spot radius R, pressure P, and central temperature T are normalized with their stagnation values (defined later) calculated without including the alpha-particle energy deposition: $\hat{R} = R/R_{\rm stag}^{\rm no\,\alpha}$, $\hat{P} = P/P_{\rm stag}^{\rm no\,\alpha}$, and $\hat{T} = T/T_*^{\rm no\,\alpha}$. The dimensionless time $\tau = tV_i/R_{\rm stag}^{\rm no\,\alpha}$ is a function of the implosion velocity V_i. Equations (1)–(3) represent the hot-spot energy balance, the temperature equation from the hot-spot mass conservation, and the thin shell Newton's law, respectively. For simplicity, we have neglected the radiation losses (included in Ref. [5]) and only retained the expansion [first term on the right hand side of (1)] and the heat conduction losses [right hand side of (2)]. The focus of this Letter is the 3-D effects included in the term $R_{\rm clean}$ in Eq. (1). The term γ_α governs the ignition conditions and can be written as

$$\gamma_\alpha = (\varepsilon_\alpha C_\sigma P_{\rm stag}^{\rm no\,\alpha} R_{\rm stag}^{\rm no\,\alpha} T_*^{\rm no\,\alpha})/(8V_i), \qquad (4)$$

where ε_α is the alpha-particle energy (3.5 MeV) and $C_\sigma \simeq 2.5 \times 10^{-26}\ {\rm m^3\,keV^{-3}\,s^{-1}}$ comes from approximating the volume integral of the fusion rate around a 4 to 15 keV central temperature with a power law $\sim T^3$. The initial conditions are defined at the time of peak implosion velocity: $P(0) = P_0$, $R(0) = R_0$, $\dot{R}(0) = -V_i$, and $T(0) = T_0$. The stagnation values $R_{\rm stag}^{\rm no\,\alpha}$, $P_{\rm stag}^{\rm no\,\alpha}$, and $T_{\rm stag}^{\rm no\,\alpha}$ are obtained by solving the dimensional form of Eqs. (1)–(3) without alpha-particle energy deposition ($\gamma_\alpha = 0$) and in the limit of large initial kinetic energy $\epsilon_0 = (M_{\rm shell}V_i^2/4\pi P_0 R_0^3) \gg 1$. This leads to the following stagnation values without alphas

$$P_{\rm stag}^{\rm no\,\alpha} \approx P_0\epsilon_0^{5/2}, \qquad R_{\rm stag}^{\rm no\,\alpha} \simeq R_0\epsilon_0^{-1/2}, \qquad (5)$$

$$T_*^{\rm no\,\alpha} \approx (1.2 P_{\rm stag}^{\rm no\,\alpha} R_{\rm stag}^{\rm no\,\alpha} V_i/\kappa_0)^{2/7}, \qquad (6)$$

where $T_*^{\rm no\,\alpha} \simeq 1.3 T_{\rm stag}^{\rm no\,\alpha}$ and $\kappa_0 \simeq 3.7 \times 10^{69}\ {\rm m^{-1}\,s^{-1}\,J^{-5/2}}$ is the coefficient of Spitzer thermal conductivity $\kappa_{\rm Sp} \approx \kappa_0 T^{5/2}$ for $\ln\Lambda \approx 5$. Using the no-α stagnation values, the initial conditions of the dimensionless model are rewritten in the simple form $\hat{P}(0) = \epsilon_0^{-5/2}$, $\hat{T}(0) = \epsilon_0^{-1/2}$, $\hat{R}(0) = \epsilon_0^{1/2}$, $\dot{\hat{R}}(0) = -1$. The ignition model comprises Eqs. (1)–(3) and the initial conditions. Ignition is defined by the critical value of the parameter γ_α in Eq. (1), yielding an explosive singular solution. In the limit of $\epsilon_0 \to \infty$, the critical value of γ_α depends solely on the effects of nonuniformities entering through the clean radius $R_{\rm clean}$. In the absence of nonuniformities, $R_{\rm clean} = R$ and the critical value of γ_α is $\gamma_\alpha(1{\rm D}) \simeq 1.1$. As the alpha heating raises the hot-spot temperature, the RT spikes are ablated by the enhanced heat flux as well as by the alpha particles leaking from the hot-spot and depositing their energy onto the spikes [8]. This causes the ablative stabilization of the RT and enhances the clean volume. This effect can be heuristically included by letting the clean radius increase up to the 1-D radius as the hot-spot temperature rises above the no-alpha value.

The aim of the new ignition model is to identify a measurable parameter describing the effects of hot-spot nonuniformities entering through the time history of the clean radius $R_{\rm clean}(\tau)$. The RT spikes first grow exponentially until reaching the saturation amplitude. After saturation, the spikes free fall into the hot spot as shown in Fig. 1; the acceleration $g(t) = R''(t)$ determines the linear growth rates $\gamma_{\rm RT} = \sqrt{kg(t)}$, where $k \sim \ell/R(t)$ is the perturbation wave number. The number of e foldings of linear growth is $n_e = \sqrt{\ell}\hat{n}_e = \int_0^{t_l}\gamma_{\rm RT}(t)dt$ where t_l is the interval of linear growth up to saturation. In the nonlinear free-fall stage, the spikes amplitude grow as $\Delta R \approx \eta(t_l) + \int_{t_l}^{t} dt' \int_{t_l}^{t'} g(t'')dt''$ where $\eta(t_l)$ is the linear amplitude at saturation. For simplicity, we assume that the linear growth can be neglected [small $\eta(t_l)$] with respect to the nonlinear growth so that the spike amplitude ΔR depends only on t_l and t. This leads to a clean radius $R_{\rm clean} = R - \Delta R = R(t_l) + R'(t_l)(t - t_l)$ for $t > t_l$. Before t_l, the clean radius equals the 1-D radius, $R_{\rm clean} \approx R$. The time t_l depends on the amplitude of the inner DT-ice roughness at the end of the acceleration phase. The larger the initial nonuniformity level, the smaller the time t_l. We first solve Eqs. (1)–(3) without alpha-particle energy deposition and compute $\hat{R}^{\rm no\,\alpha}(\tau)$. Then, we use $\hat{R}^{\rm no\,\alpha}$ to determine $\hat{R}_{\rm clean}$ using the free-fall model. The number of e foldings of linear growth is directly proportional to

$$\hat{n}_e^{\rm no\,\alpha} \approx \frac{\pi}{2} + \arctan\left(\sqrt{\epsilon_0} - \frac{\epsilon_0}{\tau_l}\right). \qquad (7)$$

For a given τ_l, we compute $\hat{n}_e^{\rm no\,\alpha}$, $R_{\rm clean}(\tau, \tau_l)$, and the yield over clean without alphas (YOC$^{\rm no\,\alpha}$)

$$\text{YOC}^{\rm no\,\alpha} = \frac{\int_0^\infty \hat{p}^2\hat{T}\hat{R}_{\rm clean}^3 d\tau}{\int_0^\infty \hat{p}^2\hat{T}\hat{R}^3 d\tau} \qquad (8)$$

where $\hat{p}$, $\hat{T}$, and $\hat{R}$ are the solutions of Eqs. (1)–(3) without alphas (i.e., $\gamma_\alpha = 0$). The YOC$^{\rm no\,\alpha}$ is the ratio of the neutron yield for a reduced clean volume to the one-dimensional neutron yield for the case without alphas. Both YOC$^{\rm no\,\alpha}$ and $\hat{n}_e^{\rm no\,\alpha}$ depend on τ_l, and a relation can be numerically derived yielding $\hat{n}_e^{\rm no\,\alpha} = \hat{n}_e^{\rm no\,\alpha}(\text{YOC}^{\rm no\,\alpha})$. Since $\hat{n}_e^{\rm no\,\alpha}$ is a measure of the initial nonuniformities, YOC$^{\rm no\,\alpha}$ can also be used to define the initial nonuniformities' level. For a given value of YOC$^{\rm no\,\alpha}$, it is possible to determine the ignition condition, including the effects of nonuniformities, by solving Eqs. (1)–(3) with alpha deposition for the corresponding clean radius $\hat{R}_{\rm clean}$ and by varying γ_α to find the critical value for a singular solution. We start by determining the transition time τ_l from linear to nonlinear growth by solving Eqs. (1)–(3) with $\hat{R}_{\rm clean} \approx \hat{R}$ (valid in the linear regime) and a given value of γ_α. The resulting radius $R^\alpha(\tau)$ is used to compute the linear e foldings

$$\hat{n}_e^{\,\alpha}(\tau_l) = \int_0^{\tau_l} \sqrt{R^{\alpha''}/R^\alpha}\, d\tau. \qquad (9)$$

This determines the time τ_l by setting $\hat{n}_e^\alpha(\tau_l) = \hat{n}_e^{\rm no\,\alpha}({\rm YOC}^{\rm no\,\alpha})$, leading to a functional relation $\tau_l = \tau_l({\rm YOC}^{\rm no\,\alpha})$. Using τ_l, the clean radius history follows from

$$\hat{R}^{\,\alpha}_{\rm clean} = \hat{R}^\alpha(\tau_l) + \hat{R}^{\alpha'}(\tau_l)(\tau - \tau_l). \qquad (10)$$

The effects of nonuniformities on ignition are studied by varying the initial level of nonuniformities through ${\rm YOC}^{\rm no\,\alpha}$, computing τ_l and finding the critical γ_α in (1) yielding a singular explosive solution. This leads to the three-dimensional ignition condition shown in Fig. 2, which can be approximated by $\gamma_\alpha({\rm YOC}^{\rm no\,\alpha})^{4/5} > 1.2$. Using the definition of γ_α in Eq. (4) and substituting the energy conservation and the shell mass at stagnation (modified to include the finite shell-thickness effects [5]), one finds that $\gamma_\alpha \sim (\rho R)^{3/4} T_*^{15/8}$, leading to the following analytic ignition condition,

$$\chi^{\rm an} \approx (\rho R_{\rm tot}^{\rm no\,\alpha})^{3/4} (T^{\rm no\,\alpha}/4.5)^{15/8} ({\rm YOC}^{\rm no\,\alpha})^\mu \approx 1, \qquad (11)$$

where $\rho R_{\rm tot}^{\rm no\,\alpha}$ is the total areal density (approximately equal to the shell areal density) in g/cm^2, $T^{\rm no\,\alpha}$ is the peak hot-spot temperature in keV, and $\mu \approx 4/5$. Equation (11) represents a measurable criterion that can be used to assess the 3-D implosion performance, provided the alpha particles do not significantly change the hydrodynamics. This is the case with surrogate deuterium D_2 and tritium-hydrogen-deuterium THD (with a few % of D [9]) as well as low-gain (<10%) DT capsules. Obviously, ignited DT capsules do not require an ignition criterion. The effect of nonuniformities enters the ignition condition through a single parameter: the YOC. The accuracy of the generalized ignition condition can be improved by including the effect of the ablative stabilization of the deceleration RT and by tuning the power indices in Eq. (11) through a set of numerical simulations.

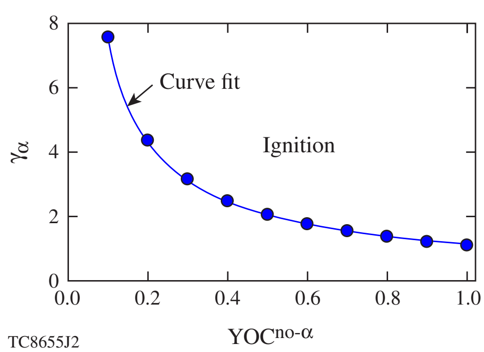

FIG. 2 (color online). The critical parameter γ_α required for a singular solution of Eqs. (1)–(3) versus the YOC. The numerical solution can be fitted by a simple power law $\gamma_\alpha \approx 1.2/({\rm YOC}^{\rm no\,\alpha})^{4/5}$.

We have carried out a set of 2-D simulations of ignition targets with varying inner ice-surface roughness using the code DRACO [10]. The initial ice roughness is increased until ignition fails. Each run is repeated without the alpha-particle energy deposition to determine the no-alpha neutron yield and the ${\rm YOC}^{\rm no\,\alpha}$. A gain curve is generated by plotting the energy gain (fusion energy yield/laser energy on target) versus the ${\rm YOC}^{\rm no\,\alpha}$. Figure 3 shows the gain curves for (a) a 420-kJ direct-drive-ignition target designed to simulate the 1-MJ indirect-drive point design [11] for the National Ignition Facility (NIF) [12], (b) the 1.5-MJ all-DT direct-drive point design [13], and (c) the 1-MJ direct-drive wetted-foam design [14].

To validate the clean-volume analysis used in the analytic ignition model, we compare the result of 2-D simulations with the same gain curve obtained from 1-D simulations, where the fusion rate $\langle\sigma v\rangle$ is reduced by a factor ξ equal to the ${\rm YOC}^{\rm no\,\alpha}$. Since the alpha-energy deposition depends on the product $\langle\sigma v\rangle V_{\rm clean}$, reducing $\langle\sigma v\rangle$ in the 1-D code by the factor $\xi = {\rm YOC}^{\rm no\,\alpha}$ is approximately equivalent to reducing the hot-spot volume by the clean-volume fraction. In the 1-D code, the reduction of $\langle\sigma v\rangle$ takes effect as long as the central hot-spot temperature is below 10 keV. For temperatures above 10 keV, the hot spot is robustly ignited, the RT becomes ablatively stabilized, and ξ is increased linearly with the temperature until $\xi = 1$ for $T > 15$ keV. This effect can also be included in the analytic model by letting $R_{\rm clean}$ approach $R_{\rm 1D}$ [in Eq. (1)] as the temperature exceeds its no-alpha value. This leads to a reduction of the YOC exponent in Eq. (11) ($\mu \approx 0.64$). Phasing out the reduction factor ξ after ignition allows the 1-D code to correctly predict the burn-wave propagation through the cold shell and the final gain. The results from the modified 1-D code are compared with the

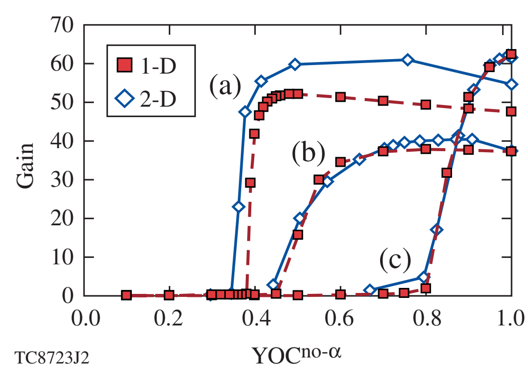

FIG. 3 (color online). Energy gain versus ${\rm YOC}^{\rm no\,\alpha}$ computed with 2-D (diamonds) and 1-D (squares) simulations. The 2-D simulations use a varying initial ice roughness. The 1-D simulations use a fusion rate reduced by the YOC to mimic the reduction of the clean hot-spot volume. The gain curves are for (a) a 420-kJ direct-drive surrogate of the 1-MJ indirect-drive NIF point design, (b) the 1.5-MJ all-DT direct-drive point design, and (c) the 1-MJ direct-drive wetted-foam design.

2-D simulations for the three targets above. As shown in Fig. 3, the modified 1-D code predicts the "ignition cliff" for critical values of the YOC$^{\text{no}\,\alpha}$ in agreement with the 2-D simulations.

The ignition cliff represents the sharp decrease in gain occurring for a critical value of the YOC. After validating the modified 1-D code with the 2-D simulations, we used the fast 1-D code to generate a database of $\rho R_n^{\text{no}\,\alpha}$, $T_n^{\text{no}\,\alpha}$, and YOC$^{\text{no}\,\alpha}$ for marginally ignited capsules with the ignition-YOC varying between 0.3 and 0.8. Marginal ignition is defined as the gain corresponding to the middle point of the ignition cliff ($\sim$ half the 1-D gain). This is a physical definition of ignition describing the onset of the burn-wave propagation. The 3-D ignition criterion based on a power law of the three measurable parameters has been derived through the best fit of the simulation results. Figure 4 shows the normalized gain curves ($G/G_{1\text{D}} =$ gain/1-D gain) from the database versus the ignition parameter χ representing the "best fit." The best fit of the ignition criterion $\chi \approx 1$ yields

$$\chi^{\text{fit}} \equiv (\rho R_{\text{tot}(n)}^{\text{no}\,\alpha})^{0.8}(T_n^{\text{no}\,\alpha}/4.7)^{1.7}(\text{YOC}^{\text{no}\,\alpha})^{\mu} \qquad (12)$$

with $\mu \approx 0.5$. This fit predicts the ignition cliff with a $\pm 10\%$ error. The subscript n indicates the spatial and temporal average with the fusion rate (i.e., neutron average) used to approximate the experimental observables. Note that T in Eq. (12) is the 1-D temperature. Since the central temperature decreases slightly with increasing nonuniformities (lower YOC), one would expect a weaker dependence on the YOC in Eq. (12) when the 2-D (or the measured) temperature is used. This is shown by the fit from a LASNEX [15] 2-D simulation database of DT and surrogate THD [9] NIF-point-design targets. A fit of the gain curves using the LASNEX database yields an ignition condition like Eq. (12) with $\mu \approx 0.4$. Cryogenic implosions on OMEGA [16] have achieved an areal density of ≈ 0.2 g/cm^2 and temperature of $\approx$2 keV with a YOC of $\approx$10% [17] leading to an ignition parameter $\chi \sim$ 0.02–0.03. Notice that the YOC$^{\text{no}\,\alpha} \equiv (Y^{\text{ex}}/Y^{1\text{D}})$ requires the 1-D yield ($Y^{1\text{D}}$) as normalization of the experimental yield (Y^{ex}). Since the 1-D yield is a strong function of the temperature, one expects a severe reduction of the temperature dependence in Eq. (12). A fit of the simulation database used in Fig. 4 shows that an approximate ignition condition ($\pm$20% error) for DT targets can be written without the temperature as

$$\rho R_{\text{tot}(n)}^{\text{no}\,\alpha}(0.1 Y_{16(no\,\alpha)}^{\text{ex}}/M_{\text{sh}}^{\text{mg}})^{0.58} \approx 1, \qquad (13)$$

where Y_{16}^{ex} is in units of 10^{16} neutrons and M_{sh} (in mg) is the portion of the shell mass stagnating at the time of peak neutron rate (bang time). For typical ICF implosions, M_{sh} is about half of the unablated shell mass. The latter can be measured or estimated from the simulations with reasonable accuracy. This result is in reasonable agreement with the analysis of Spears *et al.* [9] of the simulated downscattered neutron spectrum database for the NIF point-design target (fixed M_{sh}). An ignition condition similar to Eq. (12) can be recovered from Eq. (13) by setting $Y^{\text{ex}} =$ YOC $\cdot\, Y^{1\text{D}}$ and by using the following fit for $Y^{1\text{D}}$ of DT targets from a 1-D simulation database:

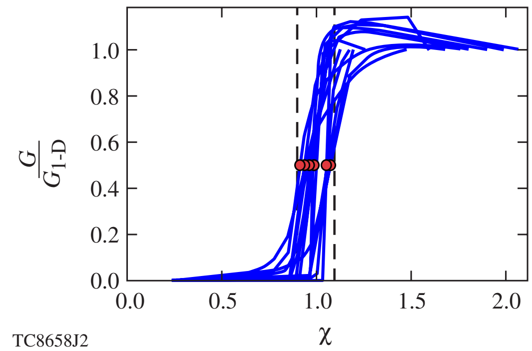

FIG. 4 (color online). Gain curves from the simulation database. The normalized gain $G/G_{1\text{-D}}$ is plotted versus the ignition parameter χ. The ignition cliff is predicted by $\chi = 1$ with a $\pm 10\%$ error.

$$Y_{16(\text{no}\,\alpha)}^{1\text{D}} \approx \left(\frac{T_n^{\text{no}\,\alpha}}{4.7}\right)^{4.7}[\rho R_{\text{tot}(n)}^{\text{no}\,\alpha}]^{0.6}\left(\frac{M_{\text{sh}}^{\text{mg}}}{0.1}\right). \qquad (14)$$

The criteria (12) and (13) are valid for central ignition and can be used to assess the performance of cryogenic implosions on the NIF and OMEGA. While the criteria are benchmarked with 2-D simulations, they are expected to be valid in 3-D. If the clean-volume analysis is correct, 3-D effects should reduce the YOC and Y^{ex} without significantly changing their exponents in (12) and (13).

This work has been supported by the U.S. Department of Energy under Cooperative Agreement No. DE-FC02-04ER54789 and No. DE-FC52-08NA28302.

[1] S. Atzeni and J. Meyer-ter-vehn, *The Physics of Inertial Fusion* (Clarendon, Oxford, 2004); J.D. Lindl, Phys. Plasmas **2**, 3933 (1995).
[2] J.D. Lawson, Proc. Phys. Soc. London Sect. B **70**, 6 (1957).
[3] M.C. Herrmann *et al.*, Nucl. Fusion **41**, 99 (2001).
[4] A. Kemp *et al.*, Phys. Rev. Lett. **86**, 3336 (2001).
[5] C. Zhou and R. Betti, Phys. Plasmas **15**, 102707 (2008).
[6] J. Garnier and C. Cherfils, Phys. Plasmas **15**, 102702 (2008).
[7] R. Kishony and D. Shvarts, Phys. Plasmas **8**, 4925 (2001).
[8] A. Schiavi and S. Atzeni, Phys. Plasmas **14**, 070701 (2007).
[9] B. Spears *et al.*, Phys. Plasmas (to be published).
[10] P. Radha *et al.*, Phys. Plasmas **12**, 056307 (2005).
[11] S.W. Haan *et al.*, Phys. Plasmas **12**, 056316 (2005).
[12] E.I. Moses, J. Phys. Conf. Ser. **112**, 012003 (2008).
[13] P.W. McKenty *et al.*, Phys. Plasmas **8**, 2315 (2001).
[14] T.J.B. Collins *et al.*, Phys. Plasmas **14**, 056308 (2007).
[15] G.B. Zimmerman and W.L. Kruer, Comments Plasma Phys. Contr. Fusion **2**, 51 (1975).
[16] T.R. Boehly *et al.*, Opt. Commun. **133**, 495 (1997).
[17] T.C. Sangster *et al.*, Phys. Rev. Lett. **100**, 185006 (2008).